Accepted Manuscript

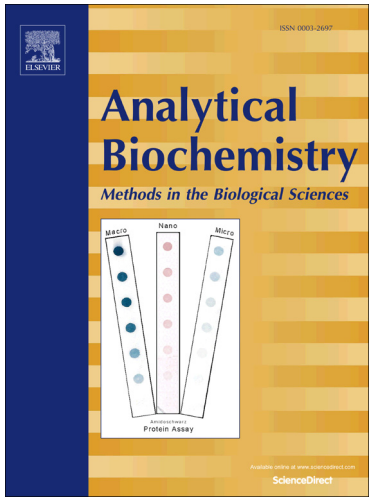

"Turn off–on" Phosphorescent Biosensors for Detection of DNA based on Quantum Dots/Acridine Orange

Yanming Miao, Yuting Li, Zhifeng Zhang, Guiqin Yan, Yi Bi

PII: S0003-2697(15)00024-X
DOI: http://dx.doi.org/10.1016/j.ab.2015.01.011
Reference: YABIO 11955

To appear in: *Analytical Biochemistry*

Received Date: 23 November 2014
Revised Date: 12 January 2015
Accepted Date: 15 January 2015

Please cite this article as: Y. Miao, Y. Li, Z. Zhang, G. Yan, Y. Bi, "Turn off–on" Phosphorescent Biosensors for Detection of DNA based on Quantum Dots/Acridine Orange, *Analytical Biochemistry* (2015), doi: http://dx.doi.org/10.1016/j.ab.2015.01.011

"Turn off–on" Phosphorescent Biosensors for Detection of DNA based on Quantum Dots/Acridine Orange

Yanming Miao [a, *] Yuting Li [a] Zhifeng Zhang [a] Guiqin Yan [a] Yi Bi [b]

[a] *Shanxi Normal University, Linfen 041004, PR China*

[b] *Yantai University, Yantai 264005, PR China*

Short title: *"Turn off–on" Phosphorescent Biosensors for DNA*

Category: *Biosensors*

[*] Corresponding author. Tel.: (86) 357-2051249; Fax.: (86) 357-2051243.
E-mail: mym8207@126.com.

Abstract: A "turn off–on" switch mode was established by using the interaction between Acridine Orange (AO) and DNA as an input signal and utilizing the room-temperature phosphorescence (RTP) reversible change of MPA-capped Mn-doped ZnS QDs (MPA: 3-mercaptopropionic acid; QDs: quantum dots) as an output signal in biological fluids. AO was absorbed into the surface of Mn-doped ZnS QDs via electrostatic attraction, and thus formed a ground-state complex through Photoinduced Electron Transfer (PIET). This complex quenched the phosphorescence of Mn-doped ZnS QDs, then rendered the system into the "turn-off" mode. Along with the addition of DNA and embedded binding with DNA, AO was competitively induced to fall off from the surface of Mn-doped ZnS QDs and embed into the double helix structure of DNA. As a result, the RTP of Mn-doped ZnS QDs was recovered and the system was rendered into "turn-on" mode consequently. In this case, a new biosensor for DNA detection was built, which has a detection limit of 0.033 mg L^{-1} and a detection range from 0.033 to 20 mg L^{-1}. What's more, such kind of biosensor does not require complex pretreatments and is free from the interference from autofluorescence and scattering light. Thus, this biosensor can be used to detect DNA in biological fluids.

Keywords: Turn off–on; Acridine orange; DNA; Biological fluids

1. Introduction

The “turn-off” switch system is commonly used for variety of sensors. However, owing to the low signal/background ratio, the application of “turn-off” mode is limited. Moreover, because of frequent nonspecific disturbance from other quenching agents, false positive results may be occurred from the “turn-off” mode. Fortunately, the shortcomings of “turn-off” switch system have been effectively overcome by the appearance of the “turn off–on” switch system, which can improve the specificity of detection systems as well [1-10]. Recently, the reversible “turn off–on” detection mode based on fluorescent quantum dots (QDs) has been successfully established [9-12], which has attracted a lot of attention and widely used in detection of DNA [12], mitoxantrone [11], nuclease [13] and virus [14, 15], and provided more reliable detection performances and specificities. Since the proportion of false positive results can be greatly reduced by the turn-on mode and a high signal/background ratio is able to be provided by fluorescent QDs, this new test mode should be further studied for future development of its application in the field of biosensors.

Recently, room-temperature phosphorescence (RTP) QDs detection has attracted much attention and has been widely applied into sensors, especially biomolecular sensors [16-27]. Owing to the longer lifetime of phosphorescence, RTP QDs detection provides high reliability and stability without interference from autofluorescence or scattered light [16, 18-20]. In additional, the detection selectivity is further enhanced as phosphorescence is less common than fluorescence [17]. The development of RTP sensors shows bright prospect [16-27] because any other complicated pretreatments are required for the developed biosensors [18, 20, 25]. However, there is rare research

about the “Turn off–on” of RTP sensors.

As a fluorescent pigment and an important nucleic acid probe, acridine orange (AO) is not only widely used to study the dynamics of DNA [28], but also commonly applied in chemistry and biology as a DNA intercalator, cell stain, and membrane penetrating probe [29-32].

As the basic genetic material in most organisms, DNA is the major carrier of genetic information and the determinant of species continuation and evolution. Even slight structural change will lead to the alteration of genetic traits and the occurrence of various diseases. Thus, research on nucleic acids has become a hotspot in biochemistry, genetics, pharmacokinetics, and other fields. Fluorescence analysis with high sensitivity, selectivity, and multiple parameters plays key roles in DNA analysis. However, the endogenous fluorescence of nucleic acids, which is very weak, cannot be used directly into the research and quantitative analysis of structures [33]. The introduction of fluorescent probes provides a powerful tool for research of nucleic acids. So far, many types of fluorescent probes have been applied into quantitative determination of nucleic acids [34-43]. The commonly-used materials include ethidium bromide [34], rare earth complexes [35-37] and cyanine dyes [38, 39]. In recent years, some nanomaterial probes including QDs have been successfully applied into detection of nucleic acids [41-43].

In this paper, we reported a novel RTP “turn off–on” switch system for sensitive DNA detection. Nanohybrids are formed by 3-Mercaptopropionic acid (MPA)-capped Mn-doped ZnS QDs and AO via electrostatic interaction, which quenched the RTP of MPA-capped Mn-doped ZnS QDs through Photoinduced Electron Transfer (PIET),

thus the RTP was "turned off". By means of intercalation with DNA, AO was competitively induced to fall off from the surface of MPA-capped Mn-doped ZnS QDs and intercalate into the double helix structure of DNA, so that the RTP of MPA-capped Mn-doped ZnS QDs can be restored and "turned on". With the increase of DNA content, the RTP restoring degree of MPA-capped Mn-doped ZnS QDs was gradually improved (Fig. 1), so we established a new biosensor for quantitative detection of DNA.

2. Experimental section

2.1. Materials and Chemicals

Mn-doped ZnS QDs were prepared from MPA (J&K Scientific, Beijing, China), $Zn(Ac)_2 \cdot 2H_2O$, $Mn(Ac)_2 \cdot 4H_2O$, and $Na_2S \cdot 9H_2O$ (Tianjing Kermel Chemical Reagent Co., China). Ultrapure water (18.2 MΩ cm) was obtained from a Water Pro water purification system (Labconco Corporation, Kansas City, MO). AO and Salmon Testes DNA (hsDNA) were provided by Sigma.

2.2. Apparatuses

The morphology and microstructure of QDs were characterized by a JEM-2100 transmission electron microscope (TEM, Japan). Phosphorescence was measured by a Cary Eclipse fluorescence spectrophotometer (Varian American Pty Ltd., America) equipped with a plotter unit and a quartz cell (1 cm × 1 cm) in the phosphorescence mode. pH was measured with a pH meter (Jinpeng Analytical Instruments Co. Ltd, China). The Resonance Light Scattering (RLS) spectra were recorded in the same spectrofluorometer by scanning both the excitation and emission monochromators (Δλ

= 0) from 200 to 700 nm. Absorption spectra were measured using a Shimadzu UV-29100 UV/Vis spectrophotometer.

2.3. Synthesis of Mn-Doped ZnS QDs

Mn-Doped ZnS QDs were synthesized in aqueous solutions as per a published method [20, 44] with minor modification. The specific steps are as follows: 5 mL of 0.1 M $Zn(Ac)_2$, 2 mL of 0.01 M $Mn(Ac)_2$, and 50 mL of 0.04 M MPA were added to a three-neck flask. With a pH meter, the mixture was adjusted to pH 11 with 1 M NaOH. At room temperature under argon conditions, after ventilation of argon for 30 min, then 5 mL of 0.1 M Na_2S was injected into the mixture. After stirring for 20 min, the solution was aged at 50 °C under open air for 2 h. The QDs were precipitated with a same volume of anhydrous ethanol and then centrifuged at 2000 r/min for 10 min. After the supernatant was discarded, the QDs were washed again with anhydrous ethanol, followed by centrifugation at 2000 r/min for another 10 min. After the supernatant was discarded, the remaining solution was vacuum-dried at room temperature for 24 h. Finally, the solid power nanoparticles as expected were prepared.

2.4. Synthesis of MPA-capped Mn-doped ZnS QDs with AO "Turn-off" nanohybrids

To study the AO effect of the MPA-capped Mn-doped ZnS QDs on the RTP intensity, we prepared a 2.0×10^{-3} M mother liquor from AO; then added different volumes of the mother liquor were added into the phosphate-buffered solution (PBS, pH 7.4, 10 mM). MPA-capped Mn-doped ZnS QDs were dissolved in water to form a 2.0 mg mL^{-1} solution, which (100 μL) was added to each of the above AO solutions.

After 5 min, the RTP was measured. RLS ($\Delta\lambda = 0$) from 200 to 700 nm in the above solutions was also detected.

2.5. Influence factors affecting Mn-doped ZnS QDs/AO nanohybrids

To investigate the effects of pH on the Mn-doped ZnS QDs/AO "Turn-off" nanohybrids, PBS solutions from pH 5.5-9.5 were prepared. The assay solutions containing MPA-capped Mn-doped ZnS QDs (100 μL), AO (50 μL), and PBS (pH 5.5-9.5) were each diluted to 5 ml. Reactions proceeded for 5 min before spectrophotometry.

To investigate the effects of retention time on the Mn-doped ZnS QDs/AO "Turn-off" nanohybrids, the assay solutions containing MPA-capped Mn-doped ZnS QDs (100 μL) and AO (50 μL) were each prepared in 5 ml of PBS (10 mM, pH 7.4). Reactions proceeded for 0, 5, 10, 20, 30, 40, or 60 min before spectrophotometry.

To investigate the effects of salt concentrations on the Mn-doped ZnS QDs/AO "Turn off" nanohybrids, the assay solutions containing MPA-capped Mn-doped ZnS QDs (100 μL), AO (50 μL), and varying concentrations of NaCl (0-0.6 M) were prepared each in 5 ml of PBS (10 mM, pH 7.4). Reactions proceeded for 5 min before spectrophotometry.

2.6. Mn-doped ZnS QDs/AO nanohybrids as RTP probe for DNA

To detect UV-vis absorption spectra of DNA, AO, Mn-doped ZnS QDs, the Mn-doped ZnS QDs/AO nanohybrids, and the Mn-doped ZnS QDs/AO + DNA; DNA (8 mg L^{-1}), AO (20 μM) and the Mn-doped ZnS QDs (40 mg L^{-1}) at different combinations were prepared each in 5 ml of PBS (10 mM, pH 7.4). Reactions proceeded for 5 min before spectrophotometry.

To study the effects of DNA on Mn-doped ZnS QDs without the presence of AO, the assay solutions containing Mn-doped ZnS QDs (100 μL) and varying concentrations of DNA (0-60 mg L^{-1}) were prepared each in 5 ml of PBS (10 mM, pH 7.4). Reactions proceeded for 5 min before spectrophotometry.

To study the DNA-AO interaction, the assay solutions containing AO (50 μL) and varying concentrations of DNA (0-80 mg L^{-1}) were prepared each in 5 ml of PBS (10 mM, pH 7.4). Reactions proceeded for 5 min before RLS detection.

2.7. DNA-AO interaction

To investigate the absorption spectra of DNA with the presence of varying concentrations of AO, we prepared solutions containing 8 mg L^{-1} DNA and 0-20 μM AO each in 5 ml of PBS (10 mM, pH 7.4). Reactions proceeded for 5 min before absorption spectral analysis.

To investigate the absorption spectra of AO with the presence of various concentrations of DNA, we prepared solutions containing 20 μM AO and 0-12 mg L^{-1} DNA each in 5 ml of PBS (10 mM, pH 7.4). Reactions proceeded for 5 min before absorption spectra analysis.

2.8. Docking calculation between salmon sperm DNA and AO

The salmon sperm DNA double-helix (CCCTAGCC) and small-molecule AO structure were constructed in SYBYL. Then the small-molecule AO was connected via the Surflex-dock module into the DNA, and the prototype molecules (default parameters) for butt-joint were formed with AT or GC as the center. Then the butting results were put out and used into analysis of the affecting mode.

2.9. Selectivity of DNA sensor

To investigate the interferences of some common metal ions and biomolecules in biological fluids, we prepared the assay solutions containing Mn-doped ZnS QDs (100 μL), AO (50 μL), DNA (1 mg L^{-1}) and varying concentrations of metal ions or biomolecules each in 5 ml of PBS (10 mM, pH 7.4). Reactions proceeded for 5 min before spectrophotometry.

2.10. Sample Pretreatment and Measurement Procedures

Urine was collected from healthy individuals, and the DNA contents were detected using the method in this system. Each determination was repeated 3 times, and the average value was computed. The specific steps are as follows: PBS (0.2 M, 0.25 mL), AO (2.0×10^{-3} M, 50 μL), MPA-capped Mn-doped ZnS QDs (2 mg mL^{-1}, 100 μL), and urine (0.05 mL) were sequentially added to a 5 mL calibrated test tube. A blank test was also set. The mixtures were diluted to 5 mL with ultrapure water, mixed thoroughly, and aged for 5 min. Then the phosphorescence of the mixtures was measured at an excitation wavelength of 295 nm. Experiments were repeated three times. Similarly, a recovery study was carried out in the samples spiked with 2.0, 3.0 and 4.0 mg L^{-1} DNA. Then the spiked recovery rate was computed as (result after spiking - result before spiking)/spiking amount. No further pretreatment procedures were employed in sample preparation.

3. Results and discussion

3.1. Characterization of the MPA-capped Mn-doped ZnS QDs

The size of MPA-capped Mn-doped ZnS QDs was tested to be about 3.5 nm by TEM (Fig. S1a). The maximum excitation peak occurred at 295 nm and a narrow emission band was centered at 590 nm: hv_1 is the fluorescence occurring from the

surface defect of ZnS QDs; hv_2 is the phosphorescence attributed to the transition of Mn^{2+} from the triplet state ($^4T_1$) to the ground state ($^6A_1$) (Fig. S1b). As reported, an orange phosphorescence emission (about 590 nm) was showed by Mn-doped ZnS QDs [45], which is attributed to the energy transfer from the band gap of ZnS to the dopant Mn^{2+} and the subsequent $^4T_1$ to $^6A_1$ transition of the Mn^{2+} incorporated into the lattice of ZnS [46].

3.2. Synthesis of MPA-capped Mn-doped ZnS QDs with AO "Turn-off" nanohybrids

With the increasing AO concentration, the RTP intensity of QDs was gradually quenched at 590 nm (Fig. 2a), and the RTP intensity became negligible with the presence of 20 μM AO (insert in Fig. 2a).

At pH 7.4, the MPA-capped Mn-doped ZnS QDs were negatively charged on surface. However, AO became a good electron acceptor and the surface of AO is positively charged since the nitrogen atoms on the heterocyclic ring of AO are prone to protonation. Therefore, Mn-doped ZnS QDs/AO nanohybrids are formed by AO and QDs based on electrostatic interaction. In order to realize the "Turn-off" mode of RTP (Fig. 2b), the PIET between AO and Mn-doped ZnS QDs quenched the RTP of Mn-doped ZnS QDs at the same time.

With addition of AO, RLS spectra show that the MPA-capped Mn-doped ZnS QDs and AO are aggregated. After that, the hydrophobic effect was enhanced, which promoted the aggregation between MPA-capped Mn-doped ZnS QDs and AO to develop larger particles (Fig. S2). Within 200-700 nm, the RLS intensity of the MPA-capped Mn-doped ZnS QDs was low. After mixing, however, with the

increase of AO concentration, the RLS intensity is also increased, which indicated that the QDs and AO formed polymers through electrostatic interaction, thus promote the aggregation via hydrophobic effect.

3.3. Factors affecting the stability of Mn-doped ZnS QDs/AO "Turn-off" nanohybrids

The effects of several factors on the RTP intensity of Mn-doped ZnS QDs/AO "Turn-off" nanohybrids were analyzed. The RTP intensity is rapidly enhanced and smoothly improved with the increment of pH within 5.5-7.0 and 7.0-8.0 respectively, and it is greatly weakened with the increase of pH within 8.0-9.0 (Fig. S3a). The reason is that, the sensor is stable within pH 7.0-8.0 when the physiological pH is 7.4, so pH 7.4 was selected as the optimal value. The RTP intensity of the "Turn-off" nanohybrids was basically stable within 60 min (Fig. S3b) or under from 0 to 0.2 M salt concentration (Fig. S3c). The above results indicate that the RTP intensity of these nanohybrids is relatively stable within pH 7.0-8.0.

3.4. Mn-doped ZnS QDs/AO nanohybrids via "Turn-on" as RTP probe for DNA

Figure 3a shows the ultraviolet (UV) spectra of DNA (curve a), AO (curve b) and MPA-capped Mn-doped ZnS QDs (curve c). With the addition of AO, enhancement and red-shift is appeared on the UV spectra of Mn-doped ZnS QDs (curved). With the addition of DNA into the mixture of Mn-doped ZnS QDs and AO, further enhancement and red-shift is appeared on the UV spectra of Mn-doped ZnS QDs (curve e). Curves d and f (data of b plus c) are very different from curves e and g (data of a plus b plus c), which indicates the obvious interactions between Mn-doped ZnS QDs and AO, and between Mn-doped ZnS QDs/AO and DNA.

The RTP intensity of Mn-doped ZnS QDs/AO nanohybrids was gradually and regularly strengthened with the increment of DNA content (Fig. 3b), and thus realize the DNA detection via the "turn-on" mode. However, with the absence of AO, the RTP intensity of separate Mn-doped ZnS QDs changed less severely with the increase of DNA content within 0 to 80 mg L^{-1}. This is because the MPA capping the surface of Mn-doped ZnS QDs and DNA are both negatively charged in a weak alkaline solution, and the interaction between DNA and Mn-doped ZnS QDs is also weak owing to mutual repelling (Fig. 3c). Figure 3d shows the RLS spectra of DNA-AO interaction. RLS was enhanced gradually with the separately fixed concentration of AO and increased concentration of DNA, which reflects the occurrence of interaction and aggregation between AO and DNA. This is mainly due to the long-distance assembly of AO on the surface of DNA molecules [47]. The large mole ratio of organic molecules to nucleic acid and the low ionic strength in the medium induced the formation of superhelix structure in nucleic acids. This superhelix structure is formed due to the long-distance assembly of organic molecules on the surface of nucleic acids. Therefore, severe increase of RLS was resulted in due to the interaction between organic molecules and nucleic acids, which indicates that organic molecules are aggregated on the surface of nucleic acids to form a superhelix structure [47, 48].

3.5. Characterization of Mn-doped ZnS QDs as RTP "Turn off–on" probes

Based on these results, a quantitative method for DNA detection by Mn-doped ZnS QDs RTP "Turn off–on" was designed. When AO and Mn-doped ZnS QDs formed nanohybrids, RTP was "turned off"; when varying contents of DNA were added into the nanohybrids, RTP was gradually recovered. Under the optimal

conditions, the RTP recovery value of the nanohybrids (ΔRTP) and the DNA concentration were in linear relationship within certain range (Fig. 4).

The linear range of DNA are 0.033-2 mg L^{-1} and 2-20 mg L^{-1}, and the linear equations are $\Delta RTP = 27.193\ C_{DNA} - 1.898$ ($R = 0.998$) and $\Delta RTP = 6.5627\ C_{DNA} - 45.432$ ($R = 0.993$). This biosensor has a detection limit (3σ) of 0.033 mg L^{-1} (where σ is the standard deviation from 11 continuous parallel detections of 0.2 mg L^{-1} DNA). For systems without DNA and with 0.2 mg L^{-1} DNA, the 11 continuous parallel detections have a relative standard deviation of 5.3%. The detection limit of this biosensor is close to that of other nanoparticle nonspecific DNA quantitative determination methods [49, 50]. But the system has a wider linear range and the RTP suffers from less background interference from biological fluids, so this system can detect DNA content in complex biological fluids without complex pretreatments.

3.6. Working mechanism between DNA and AO

The structural changes of DNA after acted with AO are an important way to study the working mechanism between DNA and AO. The action between DNA and AO was studied through UV spectra.

Figure 5a shows the UV absorption spectra of DNA molecules added with different concentrations of AO. With the increase of AO concentration, the UV absorption intensity of DNA between 210-400 nm was enhanced. With the 260nm/295nm absorption ratio (A_{260}/A_{295}) as Y-axis, and the concentration of AO as X-axis (Fig. 5b), then A_{260}/A_{295} decreased abruptly at 4 μM AO, but changed slightly with further increase of AO content. These phenomena indicate that the addition of AO can change the planar structure of DNA [19, 51-55].

Under the experimental conditions, AO was positively charged, or namely, the nitrogen atoms on its heterocyclic ring are prone to protonation. After the addition of DNA into the Mn-doped ZnS QDs/AO system, the protonated nitrogen atoms interacted electrostatically with the negatively-charged phosphate group inside the DNA. Thus, we speculate that AO and DNA were combined via intercalation.

To further confirm that DNA and AO were combined probably via intercalation, we experimentally researched the absorption spectra due to the DNA-AO interaction (Fig. 5c). Clearly, after AO interacted with DNA, the characteristic absorption peak of AO at 500 nm was bleached obviously. Such bleaching effect was probably due to the shielding effect of double chain structure of DNA on the absorbance of AO [56]. Consequently, we deduced that DNA and AO were combined probably via intercalation.

These results indicate that DNA-AO actions involved are not only electrostatic interaction, but also intercalation binding, and the action between Mn-doped ZnS QDs and AO is electrostatic interaction. Therefore, the DNA-AO interaction was stronger compared with the Mn-doped ZnS QDs/AO interaction. Thus, DNA could obtain AO from the Mn-doped ZnS QDs/AO nanohybrids, leading to the recovery of RTP in Mn-doped ZnS QD and thus to the occurrence of “turn-on”.

3.7. Docking calculation between salmon sperm DNA and AO

We simulated the docking between salmon sperm DNA and AO on SYBYL and investigated the mechanisms.

AO was inserted between the AT pair in DNA. After docking, the small-molecule puts out 20 conformations and we selected the top-ranking conformations for analysis.

We preliminarily speculated the possible combination patterns (Fig. 6A and Fig. 6B). Clearly, the optimized small-molecule was inserted between the AT pair and formed a π-π interaction together with the pyrimidine rings of adenine (A, green) and cytosine (T, red), while the electrostatic interaction was developed by protonated N atoms on AO and the DNA phosphate groups (Fig. 6A and Fig. 6B).

AO was inserted between the GC pair in DNA. After docking, the small-molecule puts out 20 conformations and we select the top-ranking conformations for analysis. We preliminarily speculate the possible combination patterns (Fig. 6C and Fig. 6D). Clearly, the optimized small-molecule was inserted mainly via π-π interaction into the GC bases, and formed a π-π action together with cytosine (C, purple) and guanine (G, blue) (Fig. 6C and Fig. 6D).

The results indicate the patterns of inserting small-molecule AO separately into the AT pair and GC pair of salmon sperm DNA, while the docking results show that the small-molecule was inserted into the DNA mainly through π-π interaction.

3.8. Selectivity of Mn-doped ZnS QDs RTP "Turn off–on" probes

Some common metal ions and biomolecules in biological fluids were used to investigate their interferences on detection of DNA by Mn-doped ZnS QDs RTP "Turn off–on" probes. With 1 mg L^{-1} DNA, the RTP change of MPA-capped Mn-doped ZnS QDs was not affected by a 2000-fold of Na^+, 500-fold of K^+, 20-fold of Ca^{2+}, 10-fold of Mg^{2+}, 100-fold Glucose, 0.2-fold RNA, 50-fold of *L*-Cys, 100-fold of *L*-His, 50-fold of *L*-Gly, 20-fold of *L*-Asp, or 15-fold of *L*-Glu.

Regarding the binding pattern, AO is embedded in between the double chains of DNA, but it is accumulated via electrostatic attraction onto the phosphate radical of

RNA. Owing to the presence of electrostatic attraction between QDs and AO and since the embedding force is stronger than the electrostatic attraction, DNA is more likely to deprive AO from the QDs, which enhances the specificity of this sensor in DNA detection.

AO can bind with both DNA and RNA, but RNA is unstable and decomposes easily in weak alkaline solutions. Thus, its content is very lower compared with DNA. In this study, the detection buffer solutions are all weak alkaline (pH 7.4); the urine solutions were further diluted by 100. As a result, the RNA content relative to DNA content can be ignored. The major reasons are listed below.

(1) Regarding the DNA decomposition enzymes, RNase is very unremovable because of its high stability and tolerance against high temperature and high pressure, while DNase will not be inactivated at high temperature. Thus, RNA stored in vitro is more prone to enzymolysis because of enzyme pollution, and should be stored under stricter conditions compared with DNA.

(2) Regarding the tolerance against acid and alkaline, RNA is more prone to decomposition under weak alkaline conditions.

(3) From the structural perspective, RNA is more prone to decomposition because its 2′ site contains a free OH, which will form an intermediate of 2′,3′-ring-shaped phosphate and requires lower free energy. On the contrary, the decomposition of DNA requires higher free energy because its 2‘ site does not contain a free hydroxy and does not produce such intermediate.

3.9. Sample analysis

Figure S4 shows that no background phosphorescence (curve 1) but strong

background fluorescence (curve 2) was found in the urine, because many proteins and other biological molecules scatter biological autofluorescence, but little autophosphorescence.

Further experiment was performed to validate whether the Mn-doped ZnS QDs RTP "Turn off–on" mode can be used in determination of DNA content. Urine was collected from healthy individuals, and the RTP was measured using the method in this system. A blank sample was also set. The difference of RTPs between the urine and the blank was computed and marked as ΔRTP, which was then substituted into $\Delta RTP = 27.193\ C_{DNA} - 1.898$ (R = 0.998). Finally, the DNA content in the urine was computed (this result corresponds to the solution diluted by 100 times, with 0.05 ml of urine). Each test was repeated 3 times. To validate the reliability of this DNA testing system in detection of urine DNA, we further tested the recovery of DNA from urine samples. Specifically, the spiking amounts of DNA were 2.0, 3.0 and 4.0 mg L^{-1} separately. The RTP after spiking was measured using the method in this system. A blank sample was also set. The difference of RTPs between the spiked urine and the blank was computed and marked as ΔRTP, which was substituted into $\Delta RTP = 6.5627\ C_{DNA} - 45.432$ (R = 0.993). The DNA content in the spiked urine was computed. The spiked recovery rate was computed as (result after spiking - result before spiking)/spiking amount. Each test was repeated 3 times. The standard addition recoveries on urine samples added with DNA are 96%-103% (Table 1). Pretreatment was not needed in all samples.

4. Conclusions

Based on the "Turn off–on" mode, a biosensor for quantitative detection of DNA in biological fluids was proposed. AO was absorbed into the surface of MPA-capped Mn-doped ZnS QDs by means of electrostatic attraction, and a ground-state complex was formed by Photoinduced Electron Transfer (PIET). Such reactions quenched the phosphorescence of QDs and developed MPA-capped Mn-doped ZnS Dots/AO nanohybrids, rendered the system into "turn off" mode. With the addition of DNA, AO was competitively induced to fall off from the surface of the QDs and embed into the double helix structure of DNA through the intercalation with DNA. Such reactions recovered the RTP of QDs and rendered the system into "turn-on" mode. Finally, we realized the "Turn off–on" of MPA-capped Mn-doped ZnS QDs by quenching and recovering RTP. Based on this, a new biosensor for DNA detection was developed. This sensor has a detection limit of 0.033 mg L^{-1} and two linear ranges from 0.033 to 2 mg L^{-1} and from 2 to 20 mg L^{-1}. The present QDs-based RTP "Turn off–on" biosensor does not need deoxidants or other inducers as required by conventional RTP detection methods, and avoids interference from autofluorescence and the scattering light of the matrix that are encountered in spectrofluorometry. Therefore, this biosensor can be used to detect the DNA content in body fluids.

Acknowledgment

This work was supported by the Fund for Construction Program of Chemical Advantage and Key discipline of Shanxi Province of China (Grant 912019).

References

[1] L. Shang, L. Zhang, S. Dong, Turn-on fluorescent cyanide sensor based on copper ion-modified CdTe quantum dots, Analyst, 134(2009) 107-113.

[2] J. Du, M. Liu, X. Lou, T. Zhao, Z. Wang, Y. Xue, et al., Highly Sensitive and Selective Chip-Based Fluorescent Sensor for Mercuric Ion: Development and Comparison of Turn-On and Turn-Off Systems, Analytical Chemistry, 84(2012) 8060-8066.

[3] B. K. McMahon, T. Gunnlaugsson, Selective detection of the reduced form of glutathione (GSH) over the oxidized (GSSG) form using a combination of glutathione reductase and a Tb (III)-cyclen maleimide based lanthanide luminescent 'switch On'assay, Journal of the American Chemical Society, 134(2012) 10725-10728.

[4] F. Yan, D. Cao, N. Yang, Q. Yu, M. Wang, L. Chen, A selective turn-on fluorescent chemosensor based on rhodamine for Hg< sup> 2+</sup> and its application in live cell imaging, Sensors Actuators B: Chem, 162(2012) 313-320.

[5] J. L. Yao, X. Gao, W. Sun, X. Z. Fan, S. Shi, T. M. Yao, A Naked-Eye On–Off–On Molecular "Light Switch" Based on a Reversible "Conformational Switch" of G-Quadruplex DNA, Inorg Chem, 51(2012) 12591-12593.

[6] A. K. Ghosh, C. Ghosh, A. Gupta, A Simple Approach To Detect Caffeine in Tea Beverages, J Agr Food Chem, 61(2013) 3814-3820.

[7] D. Huang, C. Niu, X. Wang, X. Lv, G. Zeng, "Turn-On" Fluorescent Sensor for Hg^{2+} Based on Single-Stranded DNA Functionalized Mn:CdS/ZnS Quantum Dots and Gold Nanoparticles by Time-Gated Mode, Analytical Chemistry, 85(2013) 1164-1170.

[8] J. You, H. Hu, J. Zhou, L. Zhang, Y. Zhang, T. Kondo, Novel Cellulose

Polyampholyte–Gold Nanoparticle-Based Colorimetric Competition Assay for the Detection of Cysteine and Mercury(II), Langmuir, 29(2013) 5085-5092.

[9] R. Zhang, D. Zhao, H. G. Ding, Y. X. Huang, H. Z. Zhong, H. Y. Xie, Sensitive single-color fluorescence "off-on" switch system for dsDNA detection based on quantum dots-ruthenium assembling dyads, Biosensors Bioelectron, (2014).

[10] D. Zhao, J. Li, T. Yang, Z. He, "Turn off–on" fluorescent sensor for platinum drugs-DNA interactions based on quantum dots, Biosensors Bioelectron, 52(2014) 29-35.

[11] J. Yuan, W. Guo, X. Yang, E. Wang, Anticancer Drug–DNA Interactions Measured Using a Photoinduced Electron-Transfer Mechanism Based on Luminescent Quantum Dots, Analytical Chemistry, 81(2009) 362-368.

[12] D. Zhao, W. H. Chan, Z. He, T. Qiu, Quantum Dot–Ruthenium Complex Dyads: Recognition of Double-Strand DNA through Dual-Color Fluorescence Detection, Analytical Chemistry, 81(2009) 3537-3543.

[13] T. Qiu, D. Zhao, G. Zhou, Y. Liang, Z. He, Z. Liu, et al., A positively charged QDs-based FRET probe for micrococcal nuclease detection, Analyst, 135(2010) 2394-2399.

[14] L. Chen, X. Zhang, C. Zhang, G. Zhou, W. Zhang, D. Xiang, et al., Dual-Color Fluorescence and Homogeneous Immunoassay for the Determination of Human Enterovirus 71, Analytical Chemistry, 83(2011) 7316-7322.

[15] L. Chen, X. Zhang, G. Zhou, X. Xiang, X. Ji, Z. Zheng, et al., Simultaneous Determination of Human Enterovirus 71 and Coxsackievirus B3 by Dual-Color Quantum Dots and Homogeneous Immunoassay, Analytical Chemistry, 84(2012)

3200-3207.

[16] J. M. Costa-Fernández, R. Pereiro, A. Sanz-Medel, The use of luminescent quantum dots for optical sensing, TrAC Trends in Analytical Chemistry, 25(2006) 207-218.

[17] J. M. Traviesa-Alvarez, I. Sánchez-Barragán, J. M. Costa-Fernández, R. Pereiro, A. Sanz-Medel, Room temperature phosphorescence optosensing of benzo [a] pyrene in water using halogenated molecularly imprinted polymers, Analyst, 132(2007) 218-223.

[18] Y. He, H. F. Wang, X. P. Yan, Exploring Mn-doped ZnS quantum dots for the room-temperature phosphorescence detection of enoxacin in biological fluids, Analytical chemistry, 80(2008) 3832-3837.

[19] Y. He, H. F. Wang, X. P. Yan, Self‐Assembly of Mn‐Doped ZnS Quantum Dots/Octa (3‐aminopropyl) octasilsequioxane Octahydrochloride Nanohybrids for Optosensing DNA, Chemistry-A European Journal, 15(2009) 5436-5440.

[20] P. Wu, Y. He, H. F. Wang, X. P. Yan, Conjugation of glucose oxidase onto Mn-doped ZnS quantum dots for phosphorescent sensing of glucose in biological fluids, Analytical chemistry, 82(2010) 1427-1433.

[21] W.-S. Zou, D. Sheng, X. Ge, J. Q. Qiao, H. Z. Lian, Room-temperature phosphorescence chemosensor and rayleigh scattering chemodosimeter dual-recognition probe for 2, 4, 6-trinitrotoluene based on manganese-doped ZnS quantum dots, Analytical chemistry, 83(2010) 30-37.

[22] P. Wu, L. N. Miao, H. F. Wang, X. G. Shao, X. P. Yan, A Multidimensional Sensing Device for the Discrimination of Proteins Based on Manganese‐Doped ZnS

Quantum Dots, Angewandte Chemie International Edition, 50(2011) 8118-8121.

[23] C. X. Yang, X. P. Yan, Metal–Organic Framework MIL-101 (Cr) for High-Performance Liquid Chromatographic Separation of Substituted Aromatics, Analytical chemistry, 83(2011) 7144-7150.

[24] H. B. Ren, X. P. Yan, Ultrasonic assisted synthesis of adenosine triphosphate capped manganese-doped ZnS quantum dots for selective room temperature phosphorescence detection of arginine and methylated arginine in urine based on supramolecular Mg^{2+}–adenosine triphosphate–arginine ternary system, Talanta, 97(2012) 16-22.

[25] E. Sotelo-Gonzalez, M. T. Fernandez-Argüelles, J. M. Costa-Fernandez, A. Sanz-Medel, Mn-doped ZnS quantum dots for the determination of acetone by phosphorescence attenuation, Analytica Chimica Acta, 712(2012) 120-126.

[26] H. F. Wang, Y. Y. Wu, X. P. Yan, Room-Temperature Phosphorescent Discrimination of Catechol from Resorcinol and Hydroquinone Based on Sodium Tripolyphosphate Capped Mn-Doped ZnS Quantum Dots, Analytical chemistry, 85(2013) 1920-1925.

[27] Y. Miao, Z. Zhang, Y. Gong, Q. Zhang, G. Yan, Self-assembly of manganese doped zinc sulfide quantum dots/CTAB nanohybrids for detection of rutin, Biosensors Bioelectron, 52(2014) 271-276.

[28] E. B. Brauns, C. J. Murphy, M. A. Berg, Local dynamics in DNA by temperature-dependent stokes shifts of an intercalated dye, Journal of the American Chemical Society, 120(1998) 2449-2456.

[29] S. Clerc, Y. Barenholz, A Quantitative Model for Using Acridine Orange as a

Transmembrane pH Gradient Probe, Anal Biochem, 259(1998) 104-111.

[30] A. I. Kononov, E. B. Moroshkina, N. V. Tkachenko, H. Lemmetyinen, Photophysical Processes in the Complexes of DNA with Ethidium Bromide and Acridine Orange: A Femtosecond Study, The Journal of Physical Chemistry B, 105(2001) 535-541.

[31] M. B. Lyles, I. L. Cameron, Interactions of the DNA intercalator acridine orange, with itself, with caffeine, and with double stranded DNA, Biophys Chem, 96(2002) 53-76.

[32] S. A. Krolenko, S. Y. Adamyan, T. N. Belyaeva, T. P. Mozhenok, Acridine orange accumulation in acid organelles of normal and vacuolated frog skeletal muscle fibres, Cell Biol Int, 30(2006) 933-939.

[33] S. Udenfriend, P. Zaltzman, Fluorescence characteristics of purines, pyrimidines, and their derivatives: Measurement of guanine in nucleic acid hydrolyzates, Anal. Biochem. 3 (1962) 49-59.

[34] J. B. Le Pecq, C. Paoletti, A new fluorometric method for RNA and DNA determination, Anal. Biochem. 17 (1966) 100-107.

[35] Y. X. Ci, Y. Z. Li, X. J. Liu, Selective Determination of DNA by Its Enhancement Effect on the Fluorescence of the Eu^{3+}-Tetracycline Complex, Anal. Chem. 67 (1995) 1785-1788.

[36] C. Tong, Z. Hu, W. Liu, Enoxacin–Tb^{3+} complex as an environmentally friendly fluorescence probe for DNA and its application, Talanta 71 (2007) 816-821.

[37] X. Wu, C. Guo, J. Yang, M. Wang, Y. Chen, J. Liu, The Sensitive Determination of Nucleic Acids Using Fluorescence Enhancement of

Eu^{3+}-BenzoylacetoneCetyltrimethylammonium Bromide-Nucleic Acid System, J. Fluoresc. 15 (2005) 655-660.

[38] Y. Guan, W. Zhou, X. Yao, M. Zhao, Y. Li, Determination of nucleic acids based on the fluorescence quenching of Hoechst 33258 at pH 4.5, Anal. Chim. Acta 570 (2006) 21-28.

[39] C. Q. Zhu, S. J. Zhuo, H. Zheng, J. L. Chen, D. H. Li, S. H. Li, J. G. Xu, Fluorescence enhancement method for the determination of nucleic acids using cationic cyanine as a fluorescence probe, Analyst 129 (2004) 254-258.

[40] L. Zhao, X. Wu, H. Ding, J. Yang, Fluorescence enhancement effect of morin-nucleic acid-l-cysteine-capped nano-ZnS system and the determination of nucleic acid, Analyst 133 (2008) 896-902.

[41] Y. Zhou, G. Bian, L. Wang, L. Dong, L. Wang, J. Kan, Sensitive determination of nucleic acids using organic nanoparticle fluorescence probes, Spectrochimica Acta Part A: Molecular and Biomolecular Spectroscopy 61 (2005) 1841-1845.

[42] L. Y. Wang, L. Wang, F. Gao, Z. Y. Yu, Z. M. Wu, Application of functionalized CdS nanoparticles as fluorescence probe in the determination of nucleic acids, Analyst 127 (2002) 977-980.

[43] J. Zhuang, X. Zhang, G. Wang, D. Li, W. Yang, T. Li, Synthesis of water-soluble ZnS : Mn^{2+} nanocrystals by using mercaptopropionic acid as stabilizer, Journal of Materials Chemistry, 13 (2003) 1853-1857.

[44] J. Zhuang, X. Zhang, G. Wang, D. Li, W. Yang, T. Li, Synthesis of water-soluble ZnS: Mn^{2+} nanocrystals by using mercaptopropionic acid as stabilizer, Journal of Materials Chemistry, 13(2003) 1853-1857.

[45] R. Thakar, Y. Chen, P. T. Snee, Efficient emission from core/(doped) shell nanoparticles: applications for chemical sensing, Nano letters, 7(2007) 3429-3432.

[46] J. H. Chung, C. S. Ah, D. J. Jang, Formation and distinctive decay times of surface-and lattice-bound Mn2+ impurity luminescence in ZnS nanoparticles, The Journal of Physical Chemistry B, 105(2001) 4128-4132.

[47] C. Zhi Huang, Y. Fang Li, X. Dong Liu, Determination of nucleic acids at nanogram levels with safranine T by a resonance light-scattering technique, Analytica Chimica Acta, 375(1998) 89-97.

[48] C. Z. Huang, K. A. Li, S. Y. Tong, Spectrophotometry of nucleic acids by their effect on the complex of cobalt(II) with 4-[(5-chloro-2-pyridyl)azo]-1,3-diaminobenzene, Analytica Chimica Acta, 345(1997) 235-242.

[49] Y. Li, J. Chen, C. Zhu, L. Wang, D. Zhao, S. Zhuo, et al., Preparation and application of cysteine-capped ZnS nanoparticles as fluorescence probe in the determination of nucleic acids, Spectrochimica Acta Part A: Molecular and Biomolecular Spectroscopy, 60(2004) 1719-1724.

[50] Y. Zhou, G. Bian, L. Wang, L. Dong, L. Wang, J. Kan, Sensitive determination of nucleic acids using organic nanoparticle fluorescence probes, Spectrochimica Acta Part A: Molecular and Biomolecular Spectroscopy, 61(2005) 1841-1845.

[51] T. Thomas, V. A. Bloomfield, Toroidal condensation of Z-DNA and identification of an intermediate in the B to Z transition of poly (dG-m5dC). cntdot. poly (dG-m5dC), Biochemistry-us, 24(1985) 713-719.

[52] T. Thomas, R. P. Messner, Structural specificity of polyamines in left-handed< i>

Z</i>-DNA formation: Immunological and spectroscopic studies, J Mol Biol, 201(1988) 463-467.

[53] T. Thomas, M. J. Baarsch, R. P. Messner, Immunological detection of B-DNA to Z-DNA transition of polynucleotides by immobilization of the DNA conformation on a solid support, Anal Biochem, 168(1988) 358-366.

[54] A. Petrov, D. Khalil, R. Kazaryan, I. Savintsev, B. Sukhorukov, Structural and thermodynamic features of complexes formed by DNA and synthetic polynucleotides with dodecylamine and dodecyltrimethylammonium bromide, Bioelectrochemistry, 58(2002) 75-85.

[55] Y. L. Zhou, Y. Z. Li, The interaction of poly (ethylenimine) with nucleic acids and its use in determination of nucleic acids based on light scattering, Spectrochimica Acta Part A: Molecular and Biomolecular Spectroscopy, 60(2004) 377-384.

[56] G. J. Quigley, A. H. Wang, G. Ughetto, G. Van Der Marel, J. H. Van Boom, A. Rich, Molecular structure of an anticancer drug-DNA complex: daunomycin plus d (CpGpTpApCpG), Proceedings of the National Academy of Sciences, 77(1980) 7204-7208.

Table Captions

Table 1 Recovery for the determination of DNA in urine samples (Mean ± s; n = 3).

Table 1 Recovery for the determination of DNA in urine samples (Mean ± s; n = 3).

Type of samples	DNA spiked ($mg\ L^{-1}$)	Recovery (%)
Human urine	2.0	103 ± 4
	3.0	96± 2
	4.0	101 ± 2

Figure Captions

Fig. 1. (a) Schematic illustration of fabricating Mn-doped ZnS QDs "Turn off–on" for DNA detection; (b) The structure of MPA-capped Mn-doped ZnS QDs; (c) The structure of AO.

Fig. 2. (a) AO concentration-dependent RTP emission of the 40 mg L^{-1} MPA-capped Mn-doped ZnS QDs. The inset shows the change of the RTP intensity with the increase of the AO concentration. (b) Illustration of the "Turn off" of QDs after the addition of AO. Solutions were prepared in PBS (10 mM, pH 7.4).

Fig. 3. (a) UV-vis spectra of a) DNA, b) AO, c) the MPA-capped Mn-doped ZnS QDs, d) the MPA-capped Mn-doped ZnS QDs/AO nanohybrids, e) the MPA-capped Mn-doped ZnS QDs/AO + DNA, f) data of b plus c, g) data of a plus b plus c; DNA concentration-dependent RTP emission of (b) the MPA-capped Mn-doped ZnS QDs/AO hybrids, (c) the MPA-capped Mn-doped ZnS QDs without AO, and (d) AO. Solutions were prepared in PBS (10 mM, pH 7.4).

Fig. 4. Plots of ΔRTP as a function of DNA concentration show two linear ranges. Buffer, 10 mM PBS (pH 7.4); MPA-capped Mn-doped ZnS QDs, 40 mg L^{-1}; AO, 20 μM.

Fig. 5. (a) The absorption spectra of 8 mg L^{-1} DNA in the presence of varying concentrations of AO. (b) The effect of the AO concentration on A_{260}/A_{295}. (c) The absorption spectra of 20 μM AO in the presence of varying concentrations of DNA. Solutions were prepared in PBS (10 mM, pH 7.4).

Fig. 6. (A) Image showing the combination pattern between small-molecule AO and DNA (AT); (B) Local image showing the combination of small-molecule AO onto

surface (static) of DNA (AT) pocket; (C) Image showing the combination pattern between small-molecule AO and DNA (GC); (D) Local image showing the combination of small-molecule AO onto surface (static) of DNA (AT) pocket; Colors from red to purple prepresent the strongest positve and negative electrical areas.

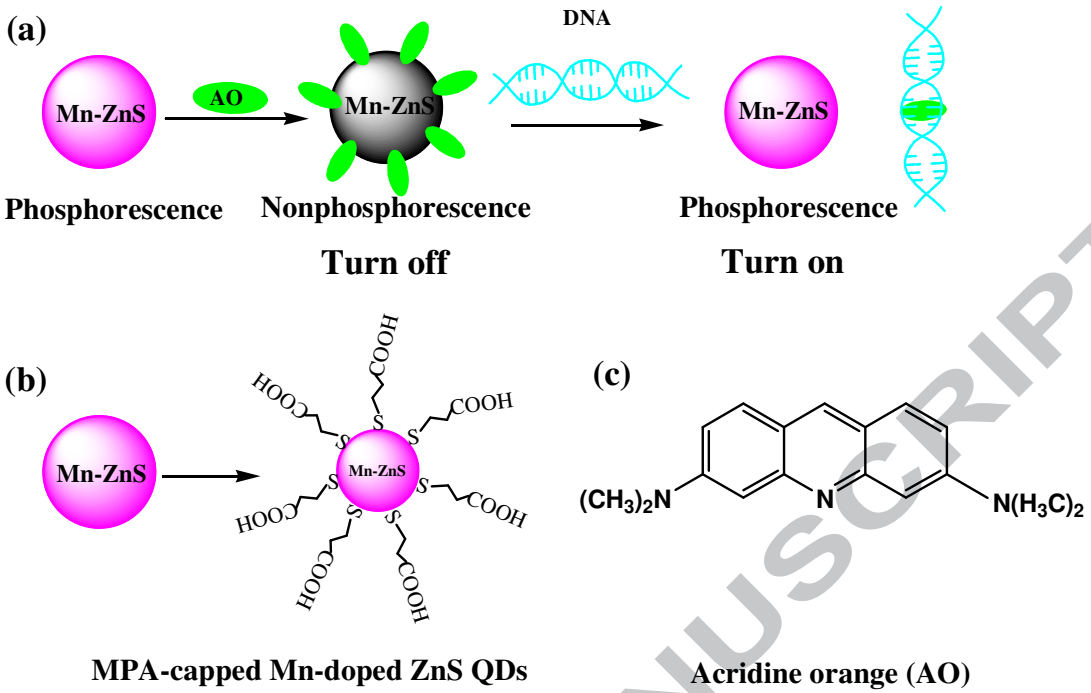

Fig. 1. (a) Schematic illustration of fabricating Mn-doped ZnS QDs "Turn off–on" for DNA detection; (b) The structure of MPA-capped Mn-doped ZnS QDs; (c) The structure of AO.

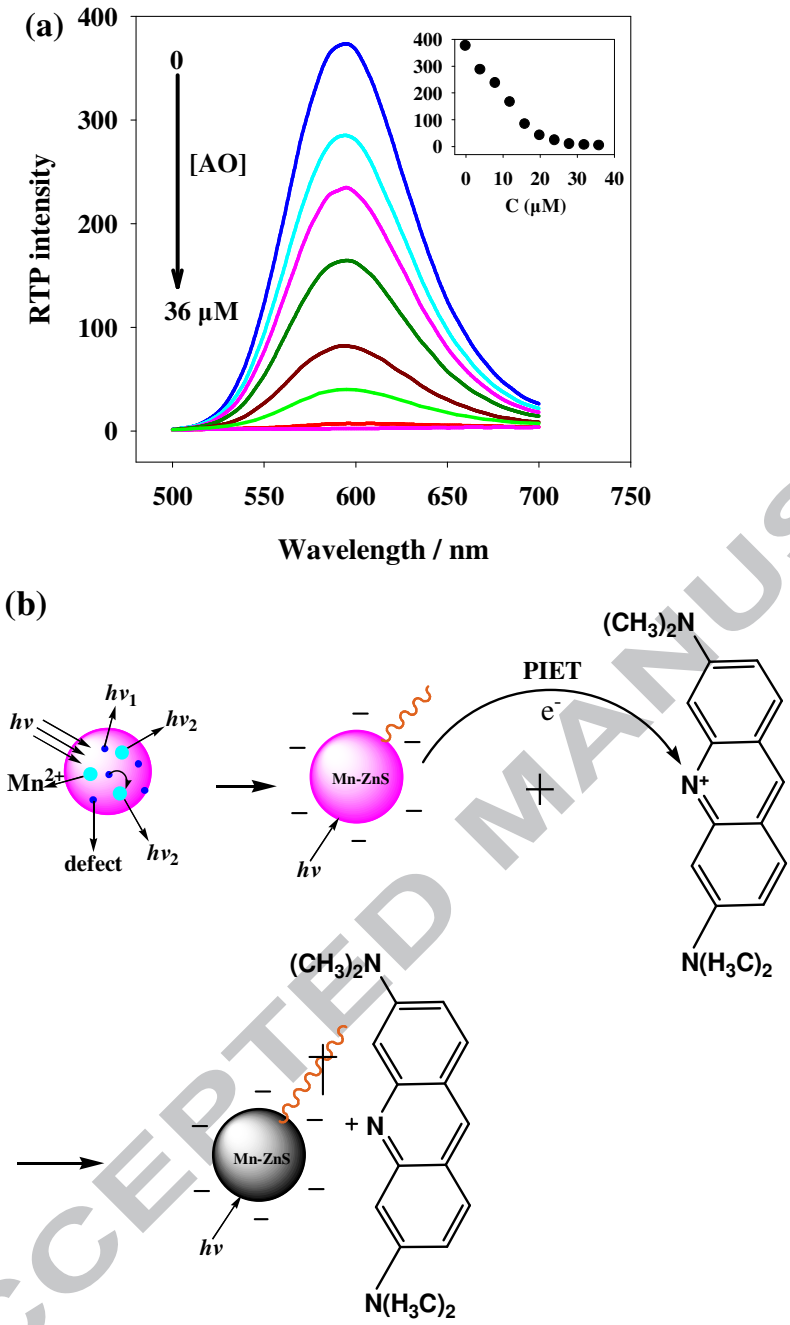

Fig. 2. (a) AO concentration-dependent RTP emission of the 40 mg L^{-1} MPA-capped Mn-doped ZnS QDs. The inset shows the change of the RTP intensity with the increase of the AO concentration. (b) Illustration of the "Turn off" of QDs after the addition of AO. Solutions were prepared in PBS (10 mM, pH 7.4).

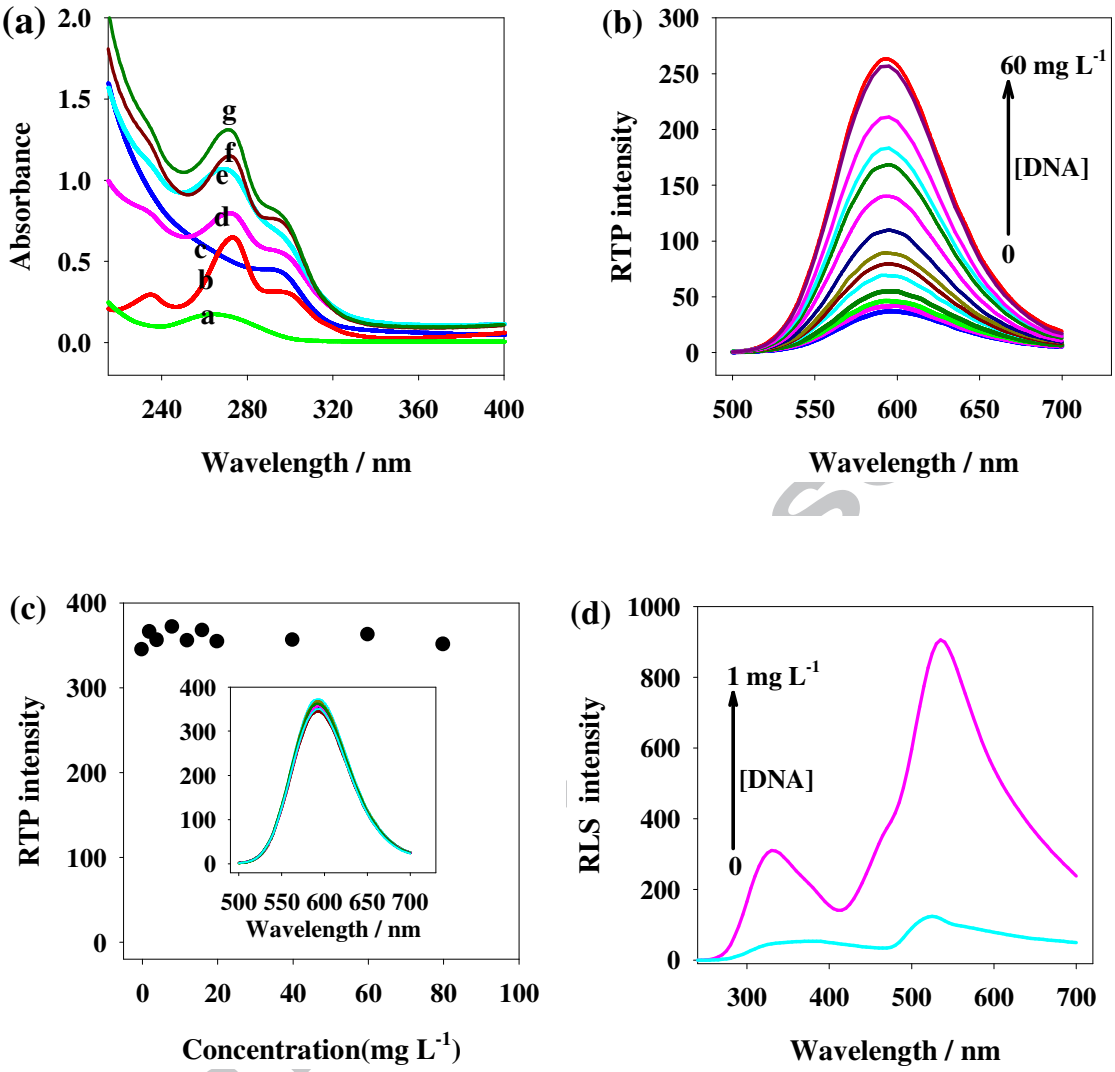

Fig. 3. (a) UV-vis spectra of a) DNA, b) AO, c) the MPA-capped Mn-doped ZnS QDs, d) the MPA-capped Mn-doped ZnS QDs/AO nanohybrids, e) the MPA-capped Mn-doped ZnS QDs/AO + DNA, f) data of b plus c, g) data of a plus b plus c; DNA concentration-dependent RTP emission of (b) the MPA-capped Mn-doped ZnS QDs/AO hybrids, (c) the MPA-capped Mn-doped ZnS QDs without AO, and (d) AO. Solutions were prepared in PBS (10 mM, pH 7.4).

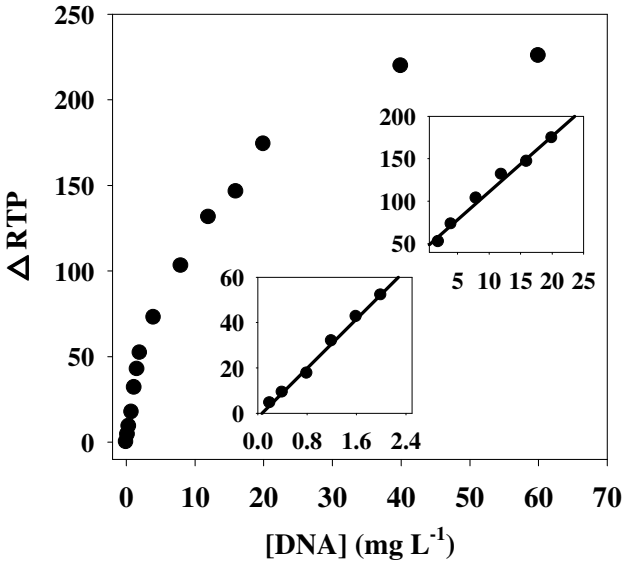

Fig. 4. Plots of ΔRTP as a function of DNA concentration show two linear ranges. Buffer, 10 mM PBS (pH 7.4); MPA-capped Mn-doped ZnS QDs, 40 mg L^{-1}; AO, 20 μM.

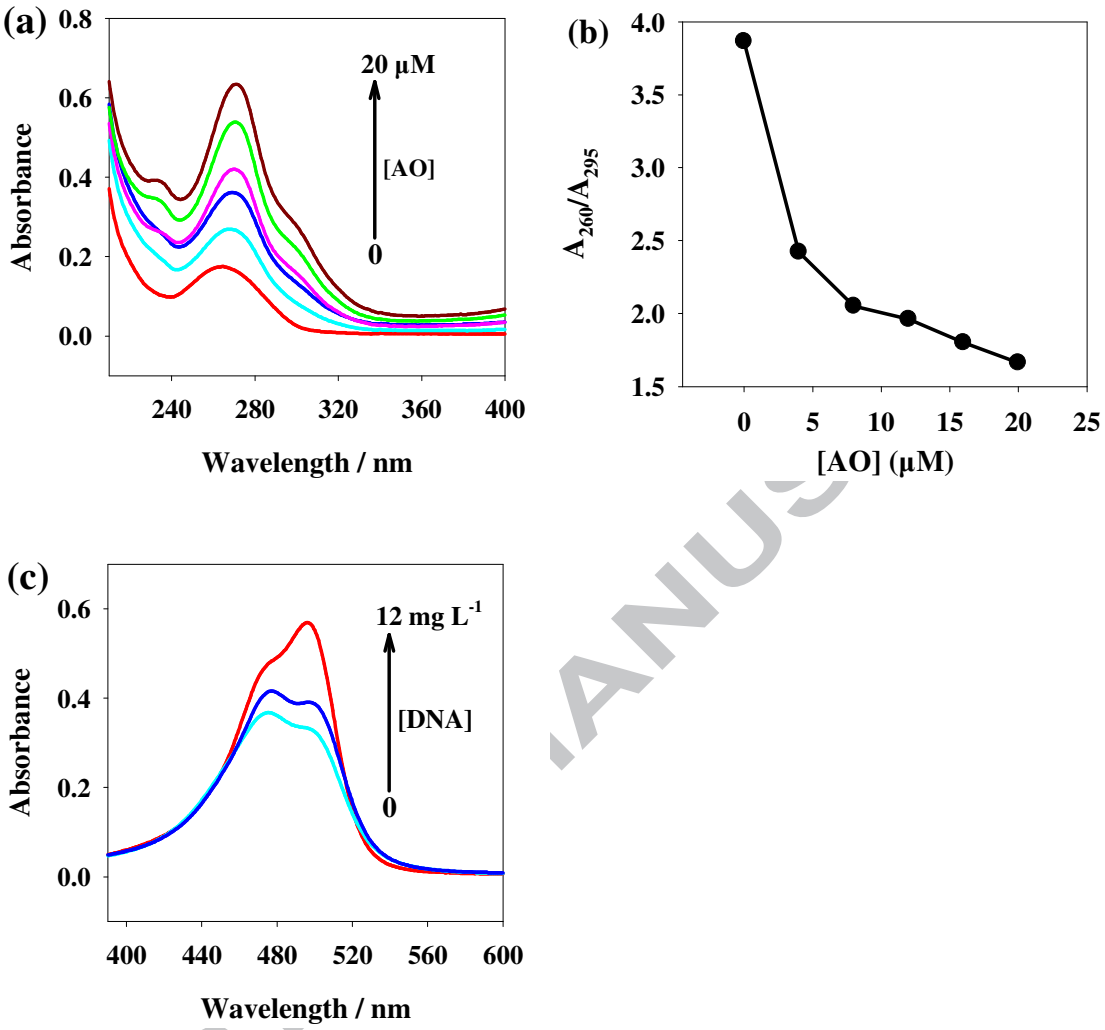

Fig. 5. (a) The absorption spectra of 8 mg L^{-1} DNA in the presence of varying concentrations of AO. (b) The effect of the AO concentration on A_{260}/A_{295}. (c) The absorption spectra of 20 µM AO in the presence of varying concentrations of DNA. Solutions were prepared in PBS (10 mM, pH 7.4).

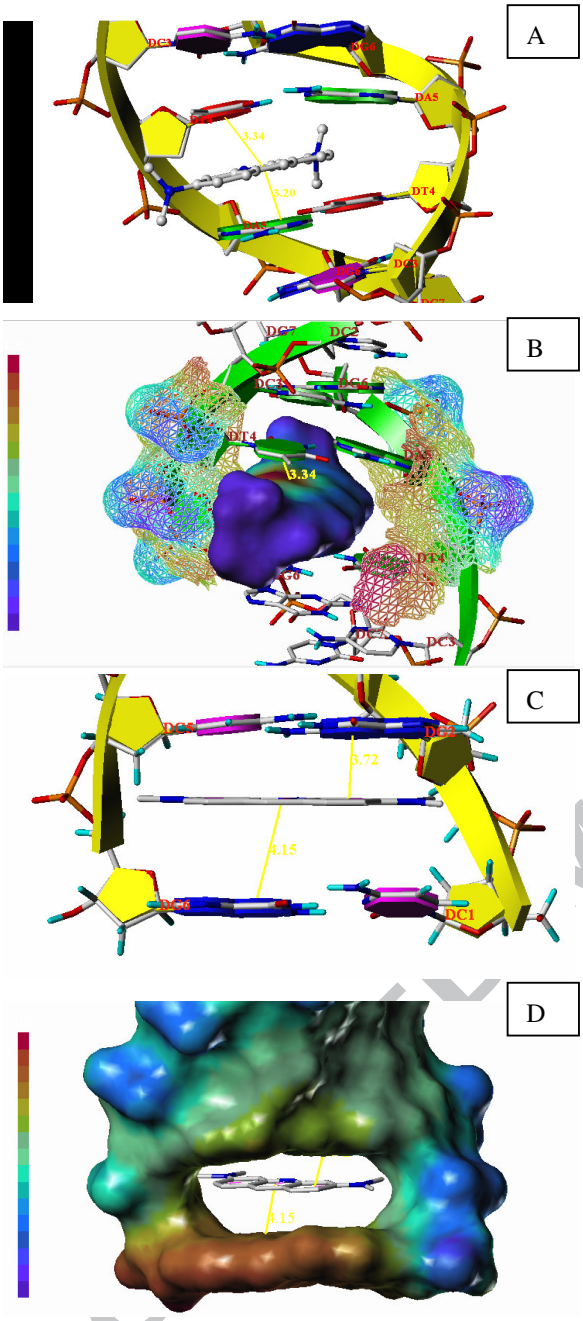

Fig. 6. (A) Image showing the combination pattern between small-molecule AO and DNA (AT); (B) Local image showing the combination of small-molecule AO onto surface (static) of DNA (AT) pocket; (C) Image showing the combination pattern between small-molecule AO and DNA (GC); (D) Local image showing the combination of small-molecule AO onto surface (static) of DNA (AT) pocket; Colors from red to purple prepresent the strongest positve and negative electrical areas.

Supplementary Materials：

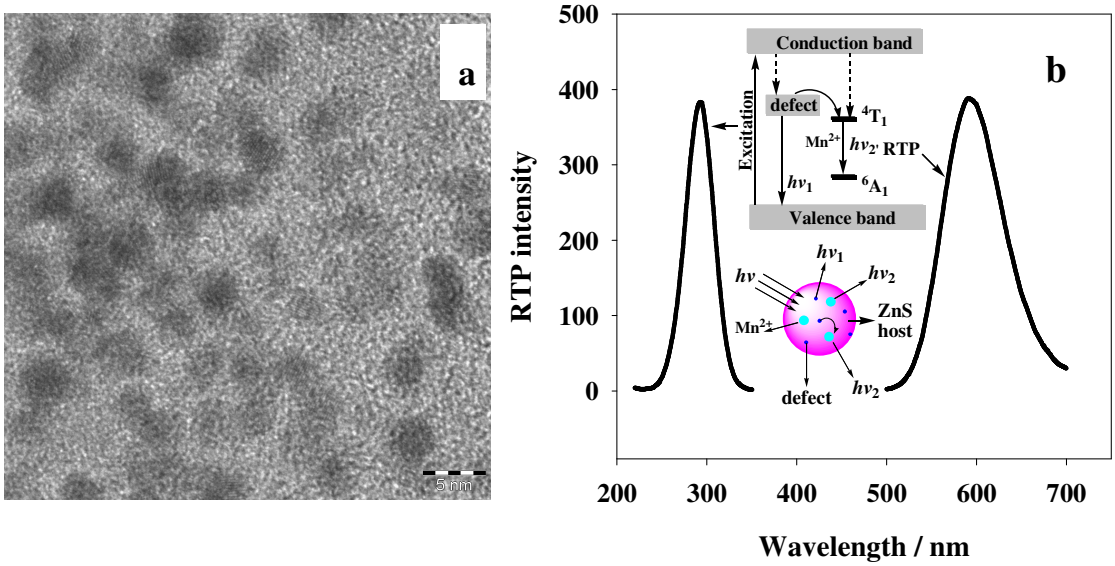

Fig. S1. (a)TEM image of MPA-capped Mn-doped ZnS QDs. (b) The excitation and RTP emission spectra of Mn-doped ZnS QDs (40 mg L^{-1}). Solutions were prepared in PBS buffer (10 mM, pH 7.4).

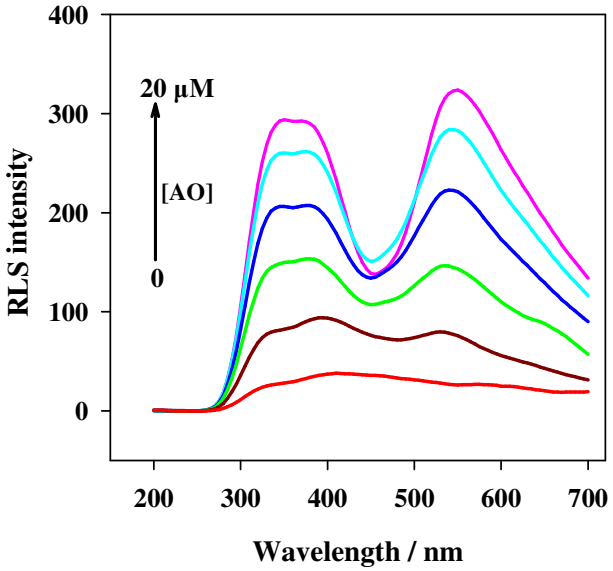

Fig. S2. RLS spectra of the MPA-capped Mn-doped ZnS QDs (40 mg L^{-1}) with the presence of varying concentrations of AO. Solutions were prepared in PBS (10 mM, pH 7.4).

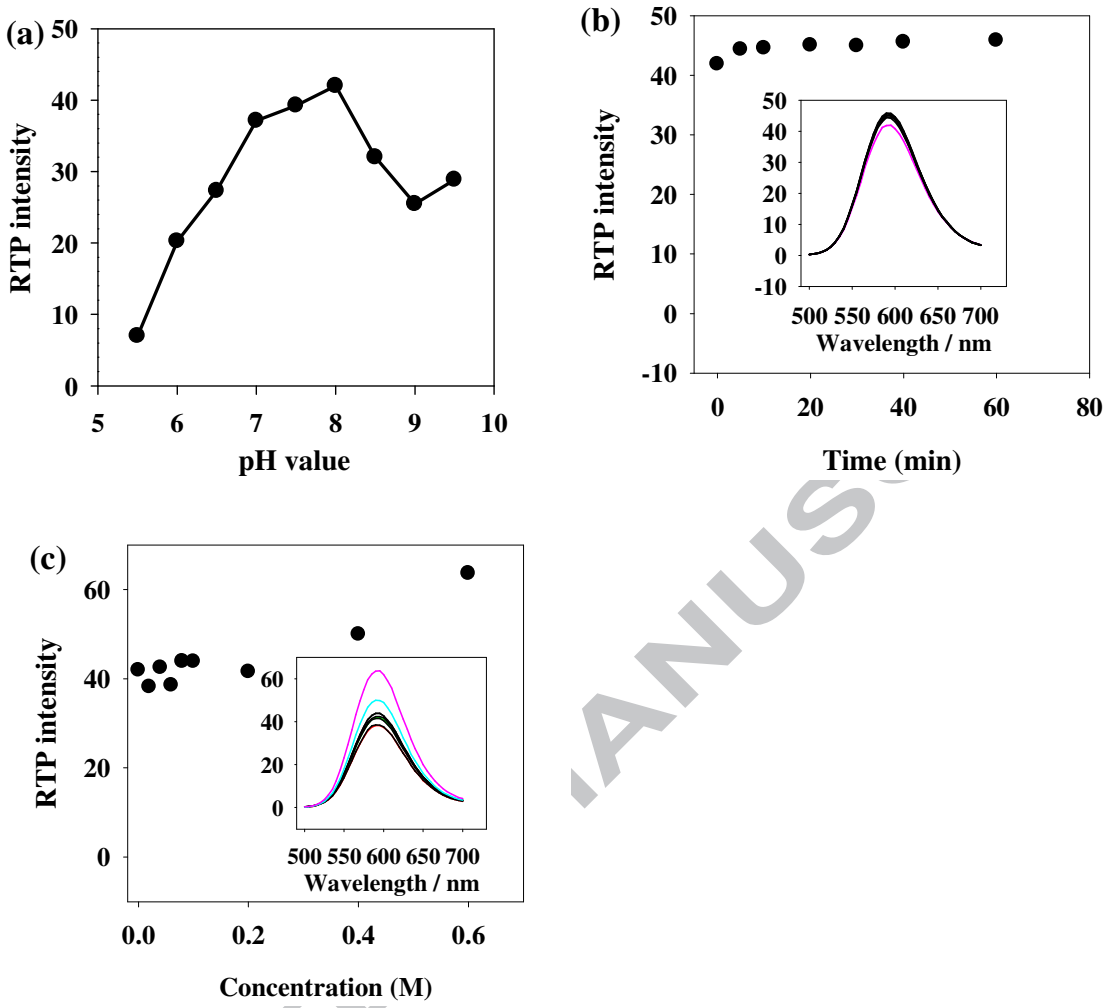

Fig. S3. (a) Effect of pH on the RTP emission of the MPA-capped Mn-doped ZnS QDs/AO. Solutions were prepared in PBS (10 mM) at different pH levels; (b) Time-dependent RTP emission of the Mn-doped ZnS QDs/AO nanohybrids. (c) Effect of NaCl concentration on the RTP emission of the Mn-doped ZnS QDs/AO (40 mg L^{-1}/20 μM) nanohybrids. Buffer: 10 mM PBS (pH 7.4).

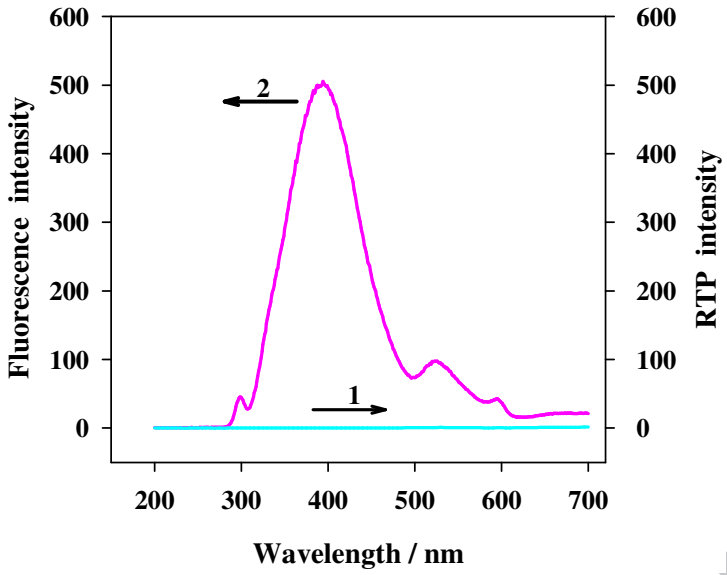

Fig. S4. The RTP (Curve 1) and fluorescence spectra (Curve 2) of urine.